The existence of a double S-shaped process curve during reactive magnetron sputtering

R. Schelfhout, K. Strijckmans, and D. Depla

Citation: Applied Physics Letters **109**, 111605 (2016); doi: 10.1063/1.4962958

View online: http://dx.doi.org/10.1063/1.4962958

View Table of Contents: http://scitation.aip.org/content/aip/journal/apl/109/11?ver=pdfcov

Published by the AIP Publishing

The existence of a double S-shaped process curve during reactive magnetron sputtering

R. Schelfhout, K. Strijckmans, and D. Depla
Department of Solid State Sciences, Ghent University, Krijgslaan 281(S1), 9000 Gent, Belgium

(Received 28 April 2016; accepted 5 September 2016; published online 16 September 2016)

The four dimensional parameter space (discharge voltage and current and reactive gas flow and pressure) related to a reactive Ar/O_2 DC magnetron discharge with an aluminum target and constant pumping speed was acquired by measuring current-voltage characteristics at different oxygen flows. The projection onto the pressure-flow plane allows us to study the well-known S-shaped process curve. This experimental procedure guarantees no time dependent effects on the result. The obtained process curve appears not to be unique but rather two significantly different S-shaped curves are noticed which depend on the history of the steady state target condition. As such, this result has not only an important impact on the fundamental description of the reactive sputtering process but it can also have its consequences on typical feedback control systems for the operation in the transition regime of the hysteresis during reactive magnetron sputtering. *Published by AIP Publishing*. [http://dx.doi.org/10.1063/1.4962958]

Reactive DC magnetron sputtering is a well-established technique to deposit compound films. Using an elemental metal target, the film composition on the substrate can be altered by controlling the reactive gas flow. However, at given sputtering conditions, an abrupt transition in the operating conditions is noticed at critical reactive gas flow rates. This instability restricts the achievable substrate compositions and/or substantially decreases the deposition rate.[1–4]

The noted Berg model[5] describing this transition in the reactive sputtering process predicts a single S-shaped process curve of the reactive partial pressure as a function of the reactive gas flow. The importance of this curve was illustrated by Kadlec *et al.*[6] showing the inherent instability of this curve under typical operating conditions, inducing the well-known hysteresis effect. Modelling this process curve yields important information on the influence of the operating variables on the hysteresis and on the deposition parameters of interest. This incentive encourages researchers to continuously improve the Berg model to account for additional effects. An important added feature is the incorporation of unbounded reactive ions in the target. This forms the core of the so-called Reactive Sputter Deposition (RSD) model.[7,8] According to this model, poisoning can also occur in an abrupt way due to an avalanche mechanism based on reactive ion implantation and the subsequently chemical reaction mechanism between these ions and target atoms. This extra mechanism comes into addition to the avalanche mechanism based on gas gettering by the deposited metal which is still the basis of the single S-shaped process curve described by other extensions to the original Berg model.[9,10]

Although the RSD model enhanced the further understanding of reactive sputtering, it also has its drawbacks compared to the Berg model. It introduces two experimentally hard to retrieve quantities: the sticking coefficient of molecular oxygen on the target surface and the reaction rate coefficient governing the reaction between the implanted reactive species and the target. This issue was however solved for the case of aluminum and yttrium in an Ar/O_2 discharge[11–13] by fitting experimental data. An interesting result from the latter work is that the steady state solution of the RSD model shows not one unique but two S-shaped process curves depending on the process history.[13] It predicts that the return to the metallic mode from the poisoned regime follows a different path as compared to the opposite transition. This phenomenon has been experimentally observed before when operating in the transition zone[14–17] but it did not receive any special attention as its origin could be linked to an irreversible change of the process parameters such as chamber heating or target erosion.

In this letter, we attempt to experimentally test the prediction of the RSD model that the reactive sputtering process is described by two S-shaped curves. This feature does not stem from time dependent effects but it originates from the fundamental nature of the target poisoning mechanism as described by the model. In order to prove this result, we introduce an alternative procedure to obtain the process curve excluding all time dependent experimental artifacts that can affect the hysteresis in an irreversible way.

A necessity in any procedure to measure the complete process curve during reactive sputtering is the possibility to operate stably in the transition zone. There are several methods to accomplish this. The hysteresis effect can be avoided by an increase of the pumping speed,[18,19] a reduction of the target area,[20] or by sputtering at higher argon pressures.[21] Also feedback mechanisms which continuously adjust the reactive gas flow[22–34] can be used to control the reactive sputtering process. An alternative and less cumbersome approach to access process conditions within the transition zone is based on a study on titanium and tantalum performed by Schiller *et al.*[25] According to this study, the control of the discharge power allows to the stable operation at any degree of target coverage. This method though boils down to controlling the discharge current due to the steep current-voltage or I–V characteristics of magnetron discharges.[26–28] Later on, McMahon *et al.*[29] noticed that in the case of Al, the system was unstable using power-controlled sputtering but

stable when the discharge voltage was controlled. This difference in behavior between Ti and Al can be understood from the material dependency of the discharge voltage on target oxidation as discussed by Depla *et al.*[30] More recently, it has been demonstrated that this voltage-controlled operating mechanism is not only applicable on small scale laboratory set-ups[31] but also on large industrial coaters.[32] We now exploit this mechanism by measuring *I–V* characteristics at constant reactive gas flow in order to investigate the hysteresis effect of aluminum.

The experiments were performed in a stainless steel vacuum chamber ($0.2 \times 0.2 \times 0.4$ m^3) which was pumped by a combination of a turbo molecular pump and a rotary pump to a base pressure of less than 1.9×10^{-5} Pa measured by a compact cold cathode gauge (Pfeiffer IKR 251). A 2 in. diameter aluminum target (Kurt J. Lesker 99.999% Al) was mounted on a home built water cooled planar magnetron as described in previous work.[30] The magnetron was powered by a Hüttinger 1500 DC power supply. A pumping speed of 30 l/s and an argon pressure of 0.4 Pa were selected to ensure a definite hysteresis behavior. The total gas pressure was measured using a capacitance gauge (Pfeiffer CMR 375). The analogue output signal of this pressure gauge was amplified by a factor of 20 to restrict the accuracy to the gauge resolution rather than the data acquisition unit. The oxygen flow was regulated using a 2 sccm (standard cubic centimeter per minute) mass flow controller (MKS M330).

During each *I–V* measurement, the oxygen flow Q was fixed and the discharge voltage V was altered with a step size of 5 V every 15 s. Meanwhile, the corresponding current I and pressure p were registered at a rate of 5 Hz. As it takes approximately 5 s until the system reaches a new steady state, only the last 10 s of each step were used for analysis. The total time interval of the voltage step (15 s) was deliberately kept short to suppress erosion effects. The necessity for a longer term stability was regularly checked by expanding the measuring period between two voltage changes. These measurements indicated that a longer time interval was not needed. The measured pressure and current within the time interval were averaged out resulting in the data points as depicted in Figure 1. The *I–V* measurement for each oxygen flow was repeated six times by increasing the discharge voltage (i.e., from poisoning towards the metallic mode) as well as by decreasing the voltage (i.e., from metallic towards the poisoned mode). All these measurements were randomly performed to exclude any systematic effect such as chamber heating. Moreover, to avoid the effects of target erosion, the discharge voltage was measured for a certain reference condition in the metallic mode. If the decrease of the voltage due to target erosion[33] exceeds 1%, a new target was mounted and sputter eroded until the reference discharge voltage was again reached. In addition, this procedure ensures a sputter cleaned metallic target surface as a starting point of each *I–V* measurement.

In order to compose a *p-Q* curve out of the (I, V, p, Q) space at a certain current (or power), it is necessary to overcome the problem that only the discharge voltage and the oxygen flow are controlled during the experiment. Hence, the values of the discharge voltage and the oxygen pressure at any discharge current (or power) must be retrieved from the data by interpolation. At first sight, one could plot the oxygen pressure as a function of the discharge current. However, the pressure is not single valued for a given current. The alternative, i.e., presenting the discharge current as a function of the oxygen pressure, is difficult due to the small experimental fluctuations in the measured oxygen pressure. Therefore, the following two-step procedure has been applied. First, the *I–V* characteristics at each flow are fitted with a B-spline curve. As the voltage was monotonously increased or decreased, the exigency for B-spline fitting is indeed satisfied. This is demonstrated in Figure 1(a) for a fixed flow of 1.2 sccm. As indicated by the grey horizontal dashed line at 0.35 A, it becomes possible now to derive the corresponding discharge voltages (indicated by blue and yellow arrows pointing downward). As a second step, the same strategy of B-spline fitting is applied to the *p-V* measurement at the same oxygen flow (see Figure 1(b)). With the derived voltages from the first step, it is then possible to derive the oxygen pressures connected to the oxygen flow at constant discharge current (indicated with arrows pointing to the left in Figure 1(b)).

By repetition of this procedure, over all six measurements per oxygen flow for both increasing and decreasing discharge voltage, an average oxygen pressure and corresponding standard deviation can be determined. In this way, it becomes possible to derive a *p-Q* process curve at constant current (here 0.35 A) as shown in Figure 2(a). It should be noted that the oxygen partial pressure is determined by subtracting the argon pressure from the total pressure. Due to experimental fluctuations, the small oxygen pressure in the metallic mode can be either positive or negative (Figure 1(b)). However, by averaging all six measurements, the oxygen pressure in the metallic mode does not differ significantly from zero.

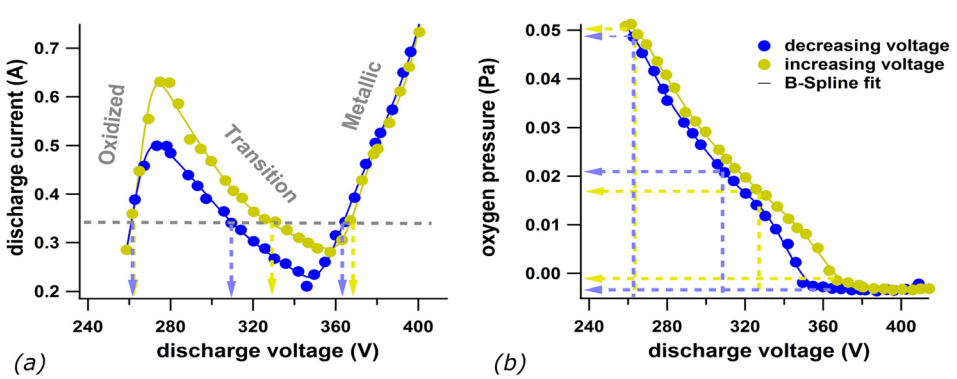

FIG. 1. An *I–V* measurement of Al with fixed oxygen gas flow (1.2 sccm). The pumping speed was set to 30 l/s and the argon pressure was 0.4 Pa. The blue markers represent a decreasing voltage (i.e., metallic to oxide), whereas the yellow markers depict an increasing voltage (i.e., oxide to metallic). The grey dashed line indicates a discharge current of 0.35 A. A double *I–V* characteristic is measured. By fitting a B-spline to (a) the *I–V* and (b) the *p-V* data, the corresponding pressure to any current can be obtained.

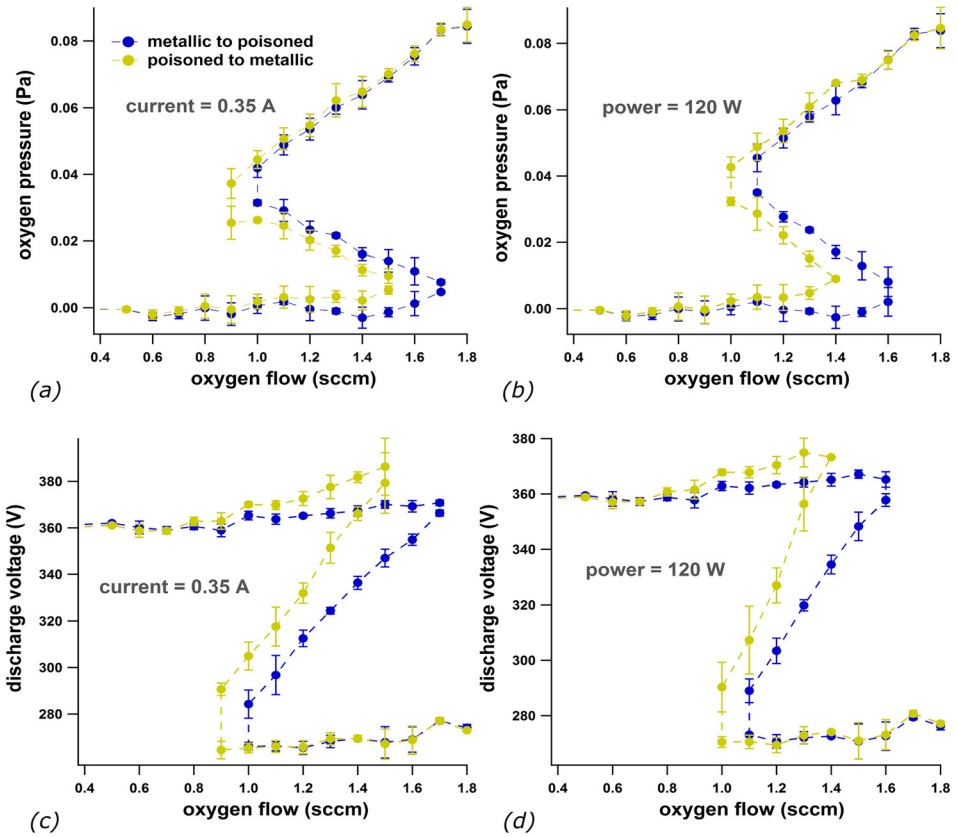

FIG. 2. The *p*-*Q* process curve for an aluminum target generated by measuring *I*–*V*-characteristics at different oxygen flows. Two different operating conditions are shown for both pressure and voltage controlled systems: (a) and (c) a constant discharge current and (b) and (d) a constant discharge power. The error bars represent the standard deviation of six identical *I*–*V* measurements.

The proposed way of data treatment permits to present the data in different ways. For example, projections such as *p*-*I* curves become possible. Many research groups perform reactive sputtering at constant power, and it is therefore interesting to show the *p*-*Q* curve not only at constant discharge currents but also at constant discharge power (see Figures 2(a) and 2(b)).

It appears that there is no unique process curve but rather two significantly different S-shaped curves which have been previously noticed before.[15,16] The double process curve is not only noticed during pressure controlled operation but also during voltage controlled which is demonstrated in Figures 2(c) and 2(d). However, it should be emphasized that due to the followed procedure, the data points of the *p*-*Q* curves are obtained from randomly performed experiments. Hence, systematic and irreversible effects such as chamber heating and target erosion can now be excluded as an explanation for the double S-shaped process curves. It could be argued that this behavior could find its origin in our specific setup. To test this possibility, the experiments were repeated in a different vacuum chamber using a cylindrical rotating magnetron. Again, a double *I*–*V* curve, similar to the result presented in Figure 1(a), is measured. This excludes the influence of the magnetron setup and/or the vacuum chamber design. An additional explanation could be a changing or even disappearing anode[34] due to the deposition of the compound on the vacuum chamber walls. Thus, a stainless steel brush was mounted as the anode ensuring a clear defined anode at any sputtering condition. These experiments yielded a double *I*–*V* curve as well. A last possible reasoning might be a difference in plasma potential. As the discharge voltage is measured between the cathode and the anode, an altering plasma potential would not be noticed. This effect should change the energy of the impinging ions and consequently the sputtering yield which would lead to a different target state. It would suggest that the double S-shaped process curve origins from the discharge and not from target poisoning mechanism as predicted by the RSD model. To investigate this reasoning, the plasma potential was measured using a Langmuir probe (Hiden Analytical ESPion). The tip of this probe was positioned perpendicular to the target surface at a distance of 10 cm to measure the plasma potential in the bulk of the plasma. Prior to each measurement, the tip was negatively biased (−100 V) to sputter clean the probe. It was found that the plasma potential of each *I*–*V* curve as shown in Fig. 1(a) only differs by 2 V. This small difference hardly changes the target state. Therefore, the shift of the discharge voltage of approximately 20 V as depicted cannot be explained by an altering plasma potential.

Hence, the result seems to be a fundamental property inherent to reactive magnetron sputtering. This implies that a correct description of the reaction kinetics of the implanted oxygen with the target material forms a crucial step in the improvement of modelling reactive sputtering. Although this seems at first sight an academic discussion, this feature also has its practical consequences to pressure-controlled feedback systems. As there are two different oxygen flows corresponding to a certain oxygen pressure, the feedback system can operate for a given set point at different flows and consequently multiple target states. It is therefore vital to any feedback mechanism to start from the same target state (either poisoned or metallic). Otherwise, reproducible operating conditions within the transition zone can be problematic.

The authors would like to acknowledge Research Foundation-Flanders (FWO) for financial support.

[1]G. Lemperiere and J. M. Poitevin, Thin Solid Films **111**, 339 (1984).
[2]Ph. Roquiny, F. Bodart, and G. Terwagne, Surf. Coat. Technol. **116–119**, 278 (1999).
[3]V. Vancoppenolle, P.-Y. Jouan, M. Wautelet, J.-P. Dauchot, and M. Hecq, J. Vac. Sci. Technol., A **17**, 3317 (1999).
[4]J. Musil, P. Baroch, J. Vlcek, K. H. Ham, and J. G. Han, Thin Solid Films **475**, 208 (2005).
[5]S. Berg, H. O. Blom, T. Larsson, and C. Nender, J. Vac. Sci. Technol., A **5**, 202 (1987).
[6]S. Kadlec, J. Musil, and H. Vyskocil, J. Phys. D: Appl. Phys. **19**, 187 (1986).
[7]D. Depla, S. Heirwegh, S. Mahieu, and R. De Gryse, J. Phys. D: Appl. Phys. **40**, 1957 (2007).
[8]D. Depla and R. Degryse, Surf. Coat. Technol. **183**, 184 (2004).
[9]S. Berg, E. Särhammar, and T. Nyberg, Thin Solid Films **565**, 186 (2014).
[10]T. Kubart, O. Kappertz, T. Nyberg, and S. Berg, Thin Solid Films **515**, 421 (2006).
[11]K. Strijckmans, W. P. Leroy, R. De Gryse, and D. Depla, Surf. Coat. Technol. **206**, 3666 (2012).
[12]K. Strijckmans, W. P. Leroy, R. De Gryse, and D. Depla, Surf. Coat. Technol. **278**, 126 (2015).
[13]K. Strijckmans, "Modelling the reactive magnetron sputtering process," Ph.D. thesis (Ghent University, 2015).
[14]K. Steenbeck, E. Steinbeiss, and K.-D. Ufert, Thin Solid Films **92**, 371 (1982).
[15]W. D. Sproul, D. J. Christie, and D. C. Carter, Thin Solid Films **491**, 1 (2005).
[16]M. Aiempanakit, T. Kubart, P. Larsson, K. Sarakinos, J. Jensen, and U. Helmersson, Thin Solid Films **519**, 7779 (2011).
[17]V. A. Marchenko, Proc. SPIE **7025**, 70250D (2008).
[18]T. Serikawa and A. Okamoto, Thin Solid Films **101**, 1 (1983).
[19]C. Li and J.-H. Hsieh, Surf. Coat. Technol. **177–178**, 824 (2004).
[20]T. Nyberg, U. Helmersson, K. Hartig, and S. Berg, Appl. Phys. Lett. **86**, 164106 (2005).
[21]E. Sarhammer, K. Strijckmans, T. Nyberg, S. Van Steenberge, S. Berg, and D. Depla, Surf. Coat. Technol. **232**, 357 (2013).
[22]W. D. Sproul, Surf. Coat. Technol. **33**, 73 (1987).
[23]A. A. Voevodin, P. Stevenson, C. Rebholz, J. M. Schneider, and M. Matthews, Vacuum **46**, 723 (1995).
[24]I. Safi, Surf. Coat. Technol. **127**, 203 (2000).
[25]S. Schiller, U. Heisig, K. Steinfelder, and J. Strümpfel, Thin Solid Films **63**, 369 (1979).
[26]J. A. Thornton, J. Vac. Sci. Technol. **15**, 171 (1978).
[27]W. D. Westwood and S. Maniv, J. Appl. Phys. **54**, 6841 (1983).
[28]A. Rizk, S. B. Youssef, and S. K. Habib, Vacuum **38**, 93 (1988).
[29]R. McMahon, J. Affinito, and R. R. Parsons, J. Vac. Sci. Technol. **20**, 376 (1982).
[30]D. Depla, S. Mahieu, and R. De Gryse, Thin Solid Films **517**, 2825 (2009).
[31]S. Cornelius, "Charge transport limits and electrical dopant activation in transparent conductive (Al,Ga):ZnO and Nb:TiO_2 thin films prepared by reactive magnetron sputtering," Ph.D. thesis (Helmholtz Zentrum Dresden, 2013).
[32]V. Linss, Surf. Coat. Technol. **290**, 43 (2016).
[33]D. Depla, S. Mahieu, J. Haemers, and R. De Gryse, Surf. Coat. Technol. **200**, 4329 (2006).
[34]J. C. Sellers, Vak. Forsch. Prax. **10**, 193 (1998).